International Journal of Chemical, Materials and Biomolecular Sciences
ISSN: 2415-6620
Vol:10, No:4, 2016

Prediction of Vapor Liquid Equilibrium for Dilute Solutions of Components in Ionic Liquid by Neural Networks

S. Mousavian, A. Abedianpour, A. Khanmohammadi, S. Hematian, Gh. Eidi Veisi

***Abstract*—**Ionic liquids are finding a wide range of applications from reaction media to separations and materials processing. In these applications, Vapor–Liquid equilibrium (VLE) is the most important one. VLE for six systems at 353 K and activity coefficients at infinite dilution (γ_i^{∞}) for various solutes (alkanes, alkenes, cycloalkanes, cycloalkenes, aromatics, alcohols, ketones, esters, ethers, and water) in the ionic liquids (1-ethyl-3-methylimidazolium bis (trifluoromethylsulfonyl)imide [EMIM][BTI], 1-hexyl-3-methyl imidazolium bis (trifluoromethylsulfonyl) imide [HMIM][BTI], 1-octyl-3-methylimidazolium bis(trifluoromethylsulfonyl) imide [OMIM][BTI], and 1-butyl-1-methylpyrrolidinium bis (trifluoromethylsulfonyl) imide [BMPYR][BTI]) have been used to train neural networks in the temperature range from (303 to 333) K. Densities of the ionic liquids, Hildebrant constant of substances, and temperature were selected as input of neural networks. The networks with different hidden layers were examined. Networks with seven neurons in one hidden layer have minimum error and good agreement with experimental data.

***Keywords*—**Ionic liquid, Neural networks, VLE, Dilute solution.

I. Introduction

IONIC liquids offer quite unique and superior properties, such as (1) high chemical stability, (2) wide liquid temperature range (approx. 300 K), (3) good solvents for polar, non-polar, organic and inorganic compounds, and (4) negligible saturation vapor-pressure and therefore non-flammability. In particular, their quite small saturation vapor pressure is desirable for green chemistry as zero emission solvents for use in environmentally friendly chemical processes. These novel solvents consist of large organic cations and anions. Because of the nearly unlimited possible combinations of cations and anions, it is possible to select a suitable ionic liquid (designersolvent) for a specific purpose. Therefore, in the last years researchers in organic chemistry, chemical engineering, electrochemistry, thermodynamics, etc. have studied ionic liquids intensively. Useful reviews are available for the usage of ionic liquids for chemical reactions [1], [2] and other industrial applications [1], [3].

S. Mousavian is with the Sama Technical and Vocational Training College, Islamic Azad University, Gachsaran Branch, Gachsaran, Iran (e-mail: S.Mousavian@iaug.ac.ir).

A. Khanmohammadi, S. Hematian, and Gh. Eidi Veisi are with the Sama Technical and Vocational Training College, Islamic Azad University, Gachsaran Branch, Gachsaran, Iran.

A. Abedianpour is with the Petrochemical Company of Gachsaran, Gachsaran, Iran.

Among the several applications foreseeable for ILs in the chemical industry there has been considerable interest in the potential of ILs for separation processes as extraction media where, among others, ILs have shown promising in the liquid–liquid extraction of organics from water [5]-[7]. One of the main ILs intrinsic attributes is the potential of tuning their physical and chemical properties and their solvating ability by varying different features of their structure, including the cation family, the cation alkyl chain length, and number of alkyl groups, and the anion identity [4].

As it is unfeasible to experimentally measure all the possible combinations of anions and cations in ILs VLE and liquid–liquid equilibrium (LLE) systems, it is essential to make measurements on selected systems to provide results that can be used to develop correlations and to test predictive methods. Several models have been used for correlating experimental data of phase equilibrium with ILs systems. Based on excess free Gibbs energy models, Wilson, UNIQUAC and original and modified UNIFAC equations have been applied to correlate solid–liquid equilibrium (SLE) and VLE of ILs systems [4], [8]-[14]. In particular, original and modified UNIFAC was also applied to correlate activity coefficients at infinite dilution and excess molar enthalpies of systems involving ILs [4], [12]. Another local composition model that proved being able to correlate data of ILs systems was the nonrandom two-liquid (NRTL) that was applied to VLE and LLE systems [4], [11], [14]-[22]. Nonetheless, correlations and group-contribution methods (GCMs) are not a good option due to the lack of a sufficiently large bank of experimental data for systems involving ILs at present. The use of equations of state (EoS) requires critical parameters of the IL, which can only be obtained indirectly and with large uncertainties [4], [23]-[25].

The aim of this research is modeling of VLE for dilute solution of ionic liquids by neural networks.

II. Experimental Data

Two different techniques [gas–liquid chromatography (g.l.c.) and dilutor technique] were used for the measurement of the activity coefficients at infinite dilution (γ_i^{∞}) in the ionic liquids. For the g.l.c. method, the solid support used as stationary phase for all measurements was Chromosorb P-AW-DMCS 60-80 mesh (acid-washed dimethyldichlorosilane-treated Chromosorb). The carrier material was coated with the desired solvent dissolved in methanol. Afterwards methanol was totally removed with the help of a rotary evaporator. Then

the column (length 250 mm, inner diameter 4.1 mm) was carefully filled with the coated solid support and the liquid loading (i.e., the amount of ionic liquid on the inert carrier material) was determined gravimetrically. A detailed scheme of the gas–liquid chromatograph and a description of the measurement procedure were already given by [26].

TABLE I
IONIC LIQUIDS INVESTIGATED IN THIS WORK

Name		Structure	
Solvent	Abbreviation	Cation	Anion
1-Hexyl-3-methyl-imidazolium bis(trifluoromethylsulfonyl)imide	[HMIM] [BTI]	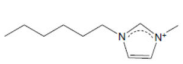	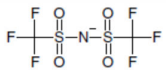
1-Octyl-3-methyl-imidazolium bis(trifluoromethylsulfonyl)imide	[OMIM] [BTI]	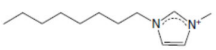	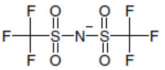
1-Butyl-1-methylpyrrolidinium bis(trifluoromethylsulfonyl)imide	[BMPYR] [BTI]	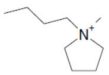	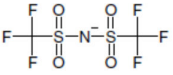

TABLE II
INFINITE DILUTION ACTIVITY COEFFICIENTS IN [HMIM][BTI]

	γ_i^∞			
	303.15 K	313.15 K	323.15 K	333.15 K
n-Pentane	5.95	5.76	5.65	5.52
n-Hexane	8.23	7.82	7.48	7.27
n-Heptane	11.2	10.6	10.0	9.67
n-Octane	15.2	14.3	13.5	13.0
1-Pentene	3.47	3.40	3.30	3.31
1-Hexene	4.71	4.61	4.48	4.44
1-Heptane	6.46	6.28	6.09	5.96
Cyclopentane	3.64	3.48	3.27	7.90
Cyclohexane	5.48	5.01	4.90	3.26
Benzene	0.75	0.76	0.78	0.79
Toluene	1.01	1.03	1.05	1.08
m-Xylene	1.40	1.41	1.46	1.50
p-Xylene	1.42	1.42	1.48	1.51
Acetone	0.31	0.32	0.34	0.34
Methanol	1.30	1.19	1.10	1.02
Ethanol	1.60	1.47	1.36	1.27
1-Propanol	1.90	1.71	1.57	1.45
2-Propanol	1.72	1.55	1.44	1.33

TABLE III
INFINITE DILUTION ACTIVITY COEFFICIENTS IN [OMIM][BTI]

	γ_i^∞			
	303.15 K	313.15 K	323.15 K	333.15 K
n-Pentane	4.07	3.94	3.78	3.60
n-Hexane	5.32	5.13	4.92	4.80
n-Heptane	6.82	6.55	6.38	6.21
n-Octane	8.92	8.43	8.14	7.82
1-Pentene	2.52	2.53	2.46	2.45
1-Hexene	3.29	3.27	3.18	3.18
1-Heptane	4.29	4.23	4.13	4.13
Cyclopentane	2.68	2.64	2.59	2.56
Cyclohexane	3.67	3.59	3.36	3.39
Benzene	0.63	0.65	0.65	0.66
Toluene	0.82	0.83	0.85	0.85
m-Xylene	1.13	1.15	1.17	1.19
o-Xylene	0.98	1.03	1.03	1.05
p-Xylene	1.11	1.13	1.16	1.16
Methanol	1.23	1.14	1.03	0.96
Ethanol	1.46	1.34	1.22	1.12
1-Propanol	1.67	1.51	1.35	1.24
Water	3.89	3.52	3.03	2.58

The determination of (γ_i^∞) using the dilutor technique was described in detail by [27]. A highly diluted solute (<0.001 mole fraction) is stripped from the solvent by the carrier gas. From the decreasing peak area with time (measured by gas chromatography), γ_i^∞ can be calculated.

The various ionic liquids investigated are shown in Table I. The experimental activity coefficients at infinite dilution (γ_i^∞) for the various solutes such as alkanes, alkenes, cycloalkanes, cycloalkenes, aromatics, alcohols, ketones, esters, ethers, and water in the ionic liquids: [HMIM][BTI], [OMIM][BTI] and [BMPYR][BTI] were measured over the temperature range (303.15 to 333.15) K and are given in Tables II-VI [1].

TABLE IV
INFINITE DILUTION ACTIVITY COEFFICIENTS IN [BMPYR] [BTI]

	γ_i^∞			
	303.15 K	313.15 K	323.15 K	333.15 K
n-Pentane	9.22	9.18	8.62	8.29
n-Hexane	13.8	13.3	12.1	11.0
n-Heptane	20.7	19.3	18.2	17.2
n-Octane	28.3	26.5	25.2	23.7
Cyclopentane	6.14	5.70	5.41	5.12
Cyclohexane	8.75	8.43	7.91	7.42
Benzene	0.84	0.86	0.88	0.89
1-Pentene	4.95	4.91	4.81	4.80
1-Hexene	7.08	6.92	6.82	6.64
1-Heptane	10.4	9.97	9.69	9.37
Ethanol	1.84	1.73	1.63	1.50
2-Propanol	2.11	1.92	1.77	1.63

TABLE V
DENSITIES FOR IONIC LIQUIDS MEASURED IN THE TEMPERATURE RANGE FROM 293 TO 358 K

Temperature (K)	Density (gr/cm^3)		
	[BMPYR] [BTI]	[HMIM] [BTI]	[OMIM] [BTI]
303.15 K	1.390	1.365	1.320
313.15 K	1.386	1.356	1.311
323.15 K	1.381	1.347	1.303
333.15 K	1.377	1.339	1.339

TABLE VI
HIDEBRANT CONSTANT OF COMPONENTS

Component	Hildebrant Constant
n-Pentane	7.020
n-Hexane	7.266
n-Heptane	7.430
n-Octane	7.551
1-Pentene	7.055
1-Hexene	7.400
1-Heptane	7.168
Cyclopentane	8.010
Cyclohexane	8.193
Benzene	9.158
Toluene	8.914
o-Xylene	8.987
m-Xylene	8.818
p-Xylene	8.769
Acetone	9.566
Methanol	14.51
Ethanol	12.915
1-Propanol	12.050
2-Propanol	11.572
Water	18.000

III. NEURAL NETWORKS

Feed-forward back-propagation artificial neural network is chosen in the present study since it is the most prevalent and generalized neural network currently in use and straightforward to implement. It has three input layer, one output layer, and one hidden layer. The neurons in hidden layer are represented by a weight matrix W, a bias vector B, a net input vector E, and an output vector O. The weights determine the strength of the connections between interconnected neurons. Every node in any hidden layer sums its weighted inputs, adds the bias constant, and then the output value of this node is calculated by applying a chosen function (known as a basis, activation, or transform function) to the weighted sum. In this manner, input values are passed through the network topology and transformed into one or more output values. The output values are then compared to the desired values to adjust the weights and bias in the nodes. Thus, the final output from the node is calculated using (1).

$$y = f\left[w_0 + \sum_{j=1}^{n_2} w_j f_j \left(\upsilon_{0j} + \sum_{i=1}^{n_1} \upsilon_{ij} x_i \right) \right] \quad (1)$$

where y is the output variable, x is input variable, w and t are the connection weights, n1 is the dimension of the input vector, and n2 is the number of hidden neurons. In this study, a sigmoid function is used as the transformation function:

$$f(x) = \frac{1}{1 + \exp(x)} \quad (2)$$

The backward propagation step calculates the error vector, E by comparing the calculated outputs, y and the target values, d by (3):

$$E = y - d \quad (3)$$

The gradient descent method is used to minimize the total error on patterns in the training set. In gradient descent, connection weights are changed in proportion to the negative of an error derivative with respect to each weight:

$$\Delta w_j = -\alpha \frac{\partial E}{\partial w_j} = \alpha \left[-\frac{\partial E}{\partial y} f'(NET) \right] x_j = \alpha \delta_y x_j \quad (4)$$

where α is a learning rate, and ∂ is an error signal. New sets of connection weights are iteratively calculated based on the error values until a minimum overall error is obtained. The connection weights are analyzed after training. These weights relate to the average contributions of each input log to the network by (5) [28]:

$$C_i = \frac{\sum_{j=1}^{n_2} w_{ij}}{\sum_{k=1}^{n_1} \sum_{j=1}^{n_2} w_{kj}} \quad (5)$$

where C_i is the average contribution of input variable i and w_{ij} is the connection weight from input neuron i to hidden neuron j. This intelligent computing technique can help engineers in solving problems that have not been solved by traditional and conventional computing methods. Neural networks do not require the specification of a structural relationship between the inputs and outputs unlike statistical regression analysis.

One of the most common problems in training an ANN is over fitting; where the error on the training set is reduced but the error for predictions using new data is large. This problem usually occurs with large networks that have few training examples. However, by dividing the data into two sets (training and testing) and selecting the best structure among them, over fitting can be avoided [28]. In the present study, 80% of the total data was used for training and testing: 60% for training and 20% for testing. The remaining 20% of the total data represented the verification or production set. The verification set is used to evaluate the accuracy of the newly built network by providing the network with a set of data that it has never seen. Prior to any modeling, all data were scaled to the range [0–1]. Once the training process converged, the testing data set was presented to the network. If the testing presented good agreement between the actual and the estimated VLE data, the bias and weight matrices were saved and kept aside. If not, the realization was canceled. This process was repeated several times until a satisfactory number

of realizations with good testing results were achieved. In this work, the network is trained for maximum 200 epochs.

IV. Results and Discussions

Compared to the development in experimental techniques, the numerical method has been improved. A feed forward back propagation network has been developed as a predicting model of VLE. It was proved that the trained network could well simulate the relation between VLE of ionic liquids as a function of temperature and properties of dissolved substance such as Hildebrant constant and density of ionic liquid. The model has been trained, validated and tested on 192 experimental data. The network with one hidden layer was selected and different neuron in hidden layer was examined. The results of different neuron in hidden layer are shown in Figs. 2 and 3.

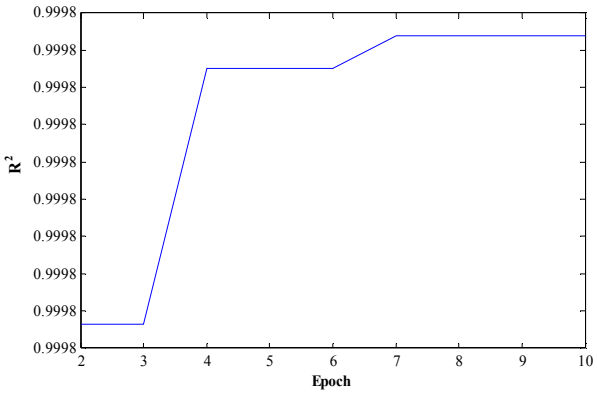

Fig. 1 Regression coefficient versus number of epoch in hidden layer

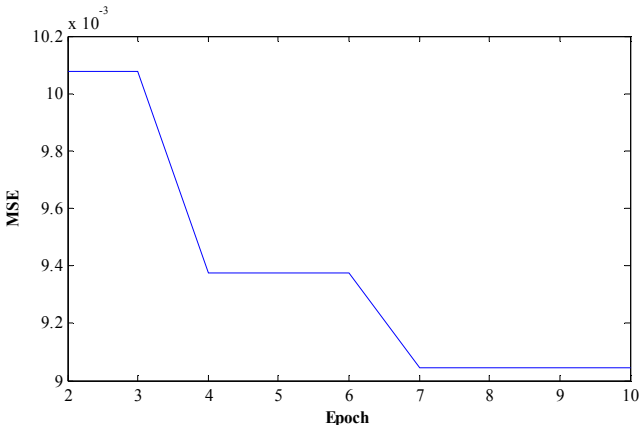

Fig. 2 Mean square error versus number of epoch in hidden layer

Figs. 1 and 2 show that neural networks with 7 neurons in one hidden layer have minimum MSE and maximum R^2. In order to avoid over fitting, the network with 7 neurons in one hidden layer was selected. The result of this network is shown in Fig. 3.

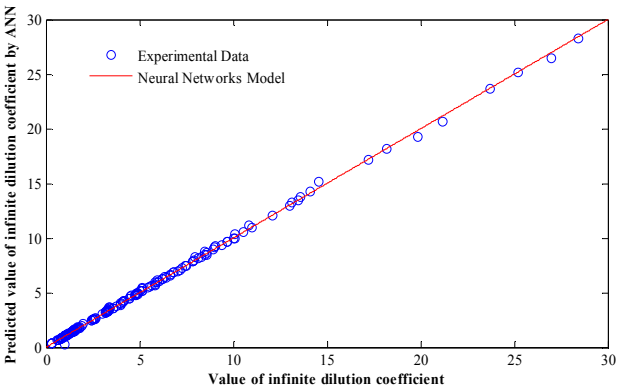

Fig. 3 Experimental and predicted value of infinite dilution coefficient

The training and testing lead to satisfactory results, the network was considered to be well trained and generalized and ready to predict the VLE.

References

[1] Ryo Kato, Jurgen Gmehling, "Systems with ionic liquids: Measurement of VLE and (γ_i^∞) data and prediction of their thermodynamic behavior using original UNIFAC, mod. UNIFAC(Do) and COSMO-RS(Ol)" , J. Chem. Thermodynamics 37 (2005) 603–619.
[2] P. Wasserscheid, T. Welton (Eds.), Ionic Liquids in Synthesis, Wiley-VCH, Weinheim, 2003.
[3] R.D. Rogers, K.R. Seddon (Eds.), Ionic Liquids – Industrial Applications for Green Chemistry, ACS Symposium Series, vol. 818, American Chemical Society, Washington, 2002.
[4] Mara G. Freire, Sonia P.M. Ventura, Luıs M.N.B.F. Santos, Isabel M. Marrucho, Joao A.P. Coutinho, " Evaluation of COSMO-RS for the prediction of LLE and VLE of water and ionic liquids binary systems" , Fluid Phase Equilibria 268 (2008) 74–84.
[5] J.G. Huddleston, H.D. Willauer, R.P. Swatloski, A.E. Visser, R.D. Rogers, Chem. Commun. 44 (1998) 1765–1766.
[6] A.G. Fadeev, M.M. Meagher, Chem. Commun. 44 (2001) 295–296.
[7] J. McFarlane,W.B. Ridenour, H. Luo, R.D. Hunt, D.W. DePaoli, D.W.R.X. Ren, Sep. Sci. Technol. 40 (2005) 1245–1265.
[8] R. Kato, J. Gmehling, Fluid Phase Equilib. 231 (2005) 38–43.
[9] U. Doman ska, E. Bogel-Łukasik, Ind. Eng. Chem. Res. 42 (2003) 6986–6992.
[10] U. Doman ska, E. Bogel-Łukasik, R. Bogel-Łukasik, Chem. Eur. J. 9 (2003) 3033–3041.
[11] M. Doker, J. Gmehling, Fluid Phase Equilib. 227 (2005) 255–266.
[12] R. Kato, J. Gmehling, J. Chem. Thermodyn. 37 (2005) 603–619.
[13] U. Domanska, Thermochim. Acta 448 (2006) 19–30.
[14] N. Calvar, B. Gonza lez, E. Gomez, A. Domı´nguez, J. Chem. Eng. Data 51 (2006) 2178–2181.
[15] T.M. Letcher, P. Reddy, Fluid Phase Equilib. 219 (2004) 107–112.
[16] T.M. Letcher, N. Deenadayalu, B. Soko, D. Ramjugernath, P.K. Naicker, J. Chem. Eng. Data 48 (2003) 904–907.
[17] S.P. Verevkin, J. Safarov, E. Bich, E. Hassel, A. Heintz, Fluid Phase Equilib. 236 (2005) 222–228.
[18] M. Bendov´ a, Z.Wagner, J. Chem. Eng. Data 51 (2006) 2126–2131.
[19] J.M. Crosthwaite, M.J. Muldoon, S.N.V.K. Aki, E.J. Maggin, J.F. Brennecke, J. Phys. Chem. B 110 (2006) 9354–9361.
[20] A. Heintz, T.V. Vasiltsova, J. Safarov, E. Bich, S.V. Verevkin, J. Chem. Eng. Data 51 (2006) 648–655.
[21] X. Hu, J. Yu, H. Liu, J. Chem. Eng. Data 51 (2006) 691–695.
[22] J. Safarov, S.P. Verevkin, E. Bich, A. Heintz, J. Chem. Eng. Data 51 (2006) 518–525.
[23] A. Shariati, C.J. Peters, J. Supercrit. Fluids 25 (2003) 109–111.
[24] L.P.N. Rebelo, J.N.C. Lopes, J.M.S.S. Esperanc¸a, E. Filipe, J. Phys. Chem. B 109 (2005) 6040–6043.
[25] J.O. Valderrama, P.A. Robles, Ind. Eng. Chem. Res. 46 (2007) 1338–1344.

[26] C. Knoop, D. Tiegs, J. Gmehling, J. Chem. Eng. Data 34 (1989) 240–247.
[27] M. Krummen, D. Gruber, J. Gmehling, Ind. Eng. Chem. Res. 39 (2000) 2114–2123.
[28] El Ouahed AK, Tiab D, Mazouzi A (2005) Application of artificial intelligence to characterize naturally fractured zones in Hassi Messaoud Oil Field, Algeria. J Pet Sci Eng 49:122–141.